JOURNAL OF SOLID STATE CHEMISTRY 69, 267–273 (1987)

# *n*-Type $SrTiO_3$ Thin Films: Electronic Processes and Photoelectrochemical Behavior

G. CAMPET,* M. CARRERE,† C. PUPRICHITKUN,* SUN ZHI WEN,* J. SALARDENNE,† AND J. CLAVERIE*

**Laboratoire de Chimie du Solide du CNRS, and †Laboratoire d'Etude des Matériauxpour la Microélectrouique, Université de Bordeaux I, 351 cours de la Libération, 33405 Talence Cedex, France*

Received June 19, 1986; in revised form November 7, 1986

Amorphous thin *n*-$SrTiO_3$ films have been prepared using the RF sputtering technique in a reductive atmosphere. Their optical absorption and photoelectrochemical properties have been investigated. In the visible region, the films display an increase of the optical absorption coefficient with wavelength, which is correlated with some deep localized levels within the band-energy gap. The low flat-band potential ($V_{fb} = -1.0$ V in 1 *M* NaOH solution) and the high ionized donor density ($N_D = 10^{20}$ cm$^{-3}$) characterize an $n^+$ degenerate semiconductor with a low electron affinity. 

## Introduction

Most of the oxide anodes investigated so far which are used in photoelectrochemical (PEC) cells are stable against photocorrosion but have low conversion efficiencies. On the other hand, efficient nonoxide converters such as Si or GaAs often show poor photoelectrochemical stability. To avoid this problem, Hodes *et al.* have focused their attention on a strategy of deposition of an inert indium tin oxide (ITO) layer on a silicon semiconductor surface so as to inhibit attack by the aqueous electrolyte (*1*). This strategy has proved to be effective, particularly for a PEC cell based on a *p*-Si substrate, yielding a 5.7% efficiency. Since the output depends on the band bending resulting from the ITO junction, an *n*-type semiconductor having an electron affinity lower than ITO should give rise to higher band bending and increase the open circuit potential. The *n*-type $SrTiO_3$ should be particularly useful for such purposes. However, whereas the properties of insulating $SrTiO_3$ thin films are very well known, no previous investigation on *n*-type $SrTiO_3$ thin films has been reported. In this paper we study the main features of *n*-type $SrTiO_3$ films (band energy gap, flat-band potential, ionized donor density, etc.) on the basis of the absorption spectra and the photoelectrochemical behavior of the corresponding electrodes. The conductivity mechanisms of the samples which vary with the preparative conditions have been reported elsewhere (*2*).

## Experimental Section

A sputtering deposition technique has been used, as it generally gives rise to highly compact films adhering tightly to the substrate.



0022-4596/87 $3.00

Thin $SrTiO_3$ films have been prepared by RF sputtering of a target (of 5 cm diameter), made of pelletized insulating $SrTiO_3$, in a reducing atmosphere. To obtain reproducible conditions the following process has been used:

-power supply: 200 W, 13 MHz
-atmosphere: *composition: Ar, 60%; $H_2$, 40%
*pressure: 1.33 Pa
-target- to- substrate distance: 4 cm
-sputtering time: 300 mn
-film thickness: 1 $\mu$m.

The substrates (1.5 × 1.5 $cm^2$, 0.02 cm thick) are either silica (for optical measurements) or tantalum plates (for photoelectrochemical determinations).

*Morphology and Texture Characterization*

The films have been analyzed by X-ray diffraction and by $\alpha$-beam nuclear analysis. Their texture was examined by SEM using a Siemens Autoscan microscope.

The optical absorption spectra were recorded with a Cary 17 ratio-recording spectrophotometer.

*Electrochemical Measurements*

Electrical contact was made onto the back side of the tantalum substrate using a silver epoxy resin. A copper wire was soldered to the contacting surface. The whole back surface was covered with an isolating epoxy resin so that only the outside surface of the deposited film was exposed to the solution.

Photoelectrochemical measurements were performed in a 1 *M* NaOH solution under potentiostatic conditions using a conventional three-electrode electrochemical cell with a large area platinium counterelectrode and a saturated calomel reference electrode (SCE). Electrode potentials were controlled by a PRT 20-2X Tacussel potentiostat and a GSTP Tacussel programmer.

The electrode was illuminated, through a quartz window introduced in the cell wall, using a 150-W high-pressure Xe lamp (Oriel) as light source whose output was passed through a monochromator (Oriel, Model 7240). The light intensity was measured with a calibrated thermopile (Kipp and Zonen, Model 754324) placed at the same position as the electrode.

## Results and Discussion

Uniform films (1 $\mu$m in thickness) with relatively smooth surface have been obtained (Fig. 1). They correspond to the expected stoichiometry as deduced from the $\alpha$-beam nuclear analysis (Fig. 2).

The X-ray diffraction patterns are indicative of partially crystallized films (Fig. 3a). However, totally crystallized films can be obtained once the samples have been heated for 5 hr at 900°C under relatively high vacuum ($10^{-6}$ Torr) (Fig. 3b). In the following the films will be designated as untreated and heat-treated samples, respectively.

*Optical Absorption and Band Energy Gap*

Figures 4a and 4b show respectively the variation in the range 300–800 nm of the transmittance as a function of photon wavelength and the calculated variation of the absorption coefficient $\alpha$. They clearly give evidence for the existence of two wavelength ranges ($\lambda > 420$ nm and $\lambda < 420$ nm).

(*i*) *High wavelength domain* ($\lambda > 420$ *nm*). In this wavelength range, $\alpha$ increases with $\lambda$ for untreated samples only (Fig. 4b, curve 1). Although this behavior could be correlated to a tailing of the conduction and valence-band edges, it also implies that deep localized levels, associated with specific defects, occur.

Either filled or empty $Sr^{2+}$ levels are too far in energy from the band gap to be relevant. Therefore $[Ti: 3d(t_{2g})]_{sub}$ and (or) $[O: 2p]_{sub}$ subband-gap energy states are responsible for the observed increase of $\alpha$

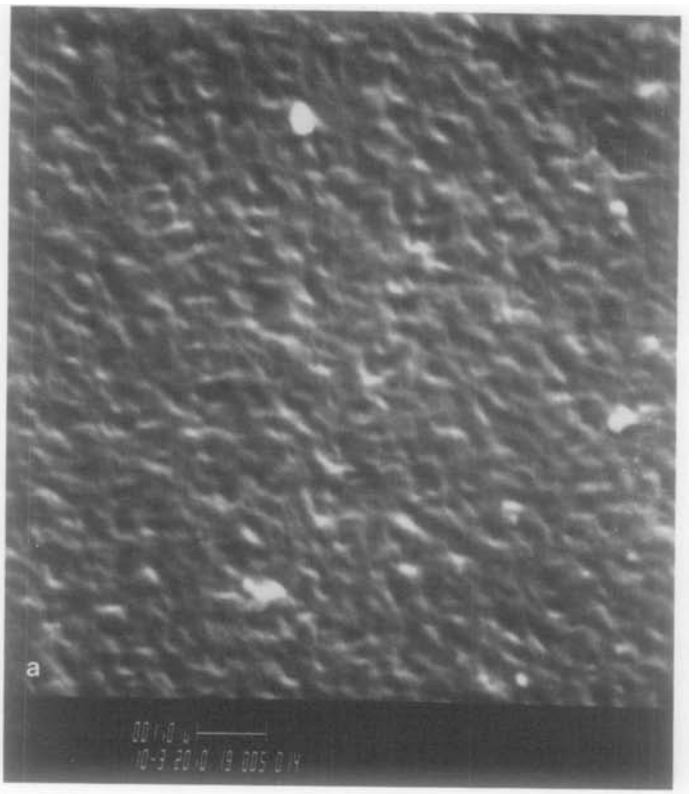


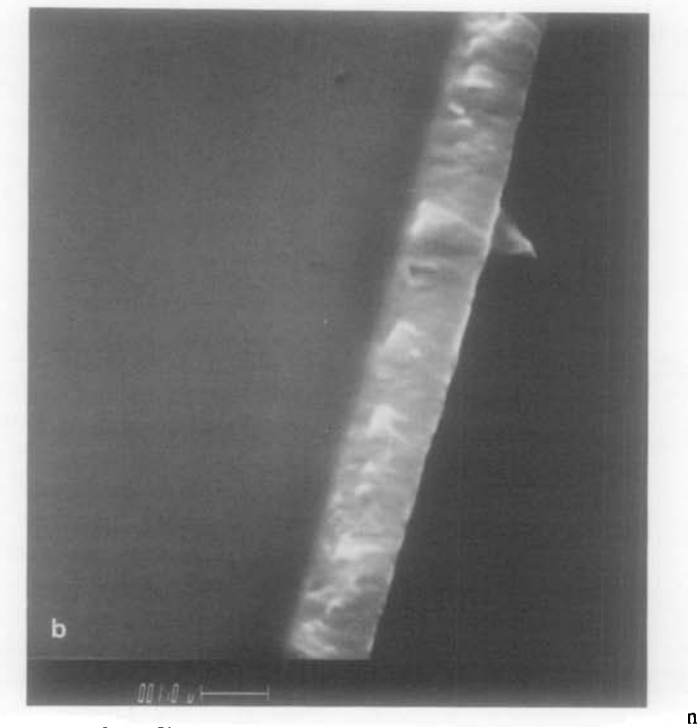


n.

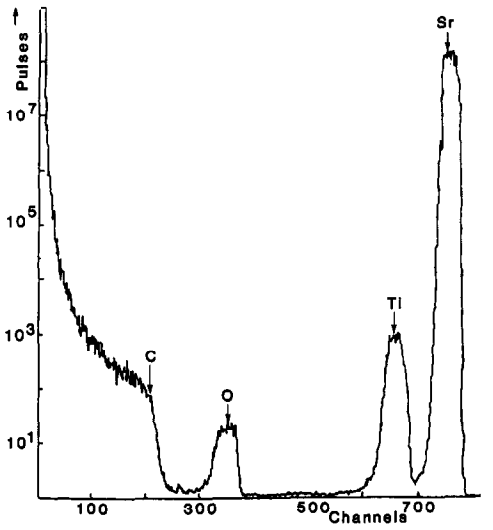


FIG. 2. $\alpha$-beam nuclear analysis of $SrTiO_3$ film deposited on graphite substrate.

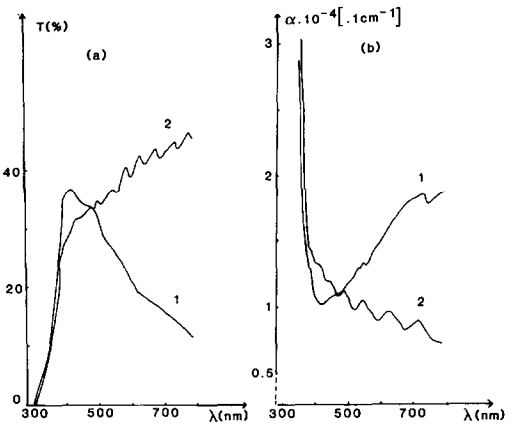


FIG. 4. Wavelength variation (a) of the transmittance and (b) of the absorption coefficient: (1) untreated films and (2) heat-treated films.

with $\lambda$ in the untreated samples. These subband-gap energy states are not likely to originate from Ti–O bond weakening, since a reduced symmetry would only introduce states near the band edges. They should rather arise from (i) titanium (oxygen) associated with oxygen (titanium) vacancies and (ii) broken Ti–O bonds.

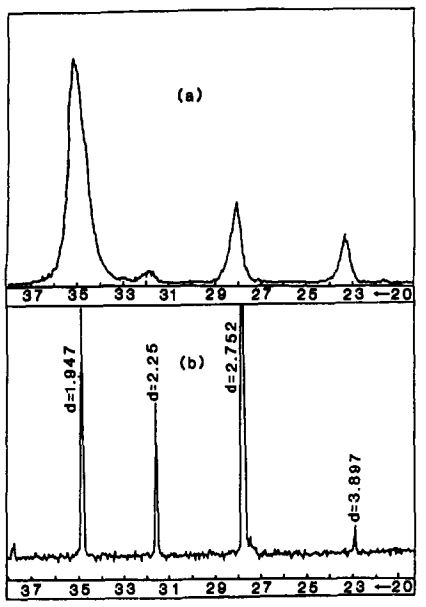


FIG. 3. X-ray diffraction patterns: (a) untreated film and (b) heat-treated film.

As previously discussed by Goodenough *et al.* for polycrystalline $SrTiO_3$ electrodes, broken titanium bonds associated with anion vacancies indeed introduce donor states, $[Ti:3d(t_{2g})]_{sub}$, lowered away from the $\pi^*$ conduction band of $Ti^{4+}:3d(t_{2g})$ parentage. Aside from these broken oxygen bonds, which occur at cation vacancies, and which introduce acceptor states, $[O:2p]_{sub}$ lifted out of the $O^{2-}:2p^6$ valence band (*4*).

In fact, the Ti–O broken bonds can be reasonably likened to the dangling bonds occurring in amorphous semiconductors such as silicon. The electron energy levels of the dangling bonds indeed constitute deep states. They can often be analyzed according to the Davis and Mott model (*5*); then they contribute to subband-gap absorption processes similar to those observed in Fig. 4-1.

On the other hand, the annealing procedure provides the thermal energy required for structuring the lattice and thus for the healing of the defects. The partially amorphous network of untreated films is then

progressively reconstructed in a manner that leads to crystallized heat-treated films. In such well-organized structures the $\alpha$ vs $\lambda$ curves are consistent with the ordinary behavior: $\alpha$ decreases as $\lambda$ increases (Fig. 4b, curve 2). The fringes encountered for these films (curves 2 in Figs. 4a and 4b) result from multireflection phenomena (interference effect) occurring both at the substrate/film and at the film/air interfaces (*3*). Their analysis, using Manifacier's model, has been reported elsewhere (*2*).

(*ii*) *Low wavelength domain* ($\lambda < 420$ *nm*): *Determination of the band-energy gaps*. Both untreated and heat-treated samples exhibit a similar variation of the absorption coefficient.

Johnson has shown that the optical absorption for interband transitions, in a crystallized semiconductor, close to the band-energy gap varies as (*6*)

$$(\alpha h\nu)^{2/n} = A(h\nu - E_g), \qquad (1)$$

where $n$ equals 1 or 4 respectively for direct or indirect transitions.

Relation (1), corresponding to $n = 4$, also applies to amorphous semiconductors (*7*).

A plot of $(\alpha h\nu)^{2/n}$ against $h\nu$ permits the determination of both $E_g$ and the nature of the transition.

Figure 5a shows the variation $(\alpha h\nu)^{1/2}$ as a function of $h\nu$ to be linear, for both untreated and heat-treated samples; thus, although $\alpha$ is large ($\alpha > 10^4$ cm$^{-1}$), the transitions are indirect, as expected, for $SrTiO_3$.

The intercept with the $h\nu$ axis yields for both samples the same $E_g$ value (3.2 eV) generally observed for $SrTiO_3$ (*7*).

### *Photoelectrochemical Behavior: Flat-Band-Potential and Ionized Donor Density*

Attention is directed to the photocurrent efficiency calculated from

$$\eta = \frac{i_l - i_d}{\phi_0}, \qquad (2)$$

where $i_l$ and $i_d$ are the respective current densities under illumination and in the dark. $\phi_0$ represents the photon flux absorbed by the electrode.

The flat-band potential $V_{fb}$ can be estimated from the theory of the depletion layer photoeffect developed by Gärtner (*9*):

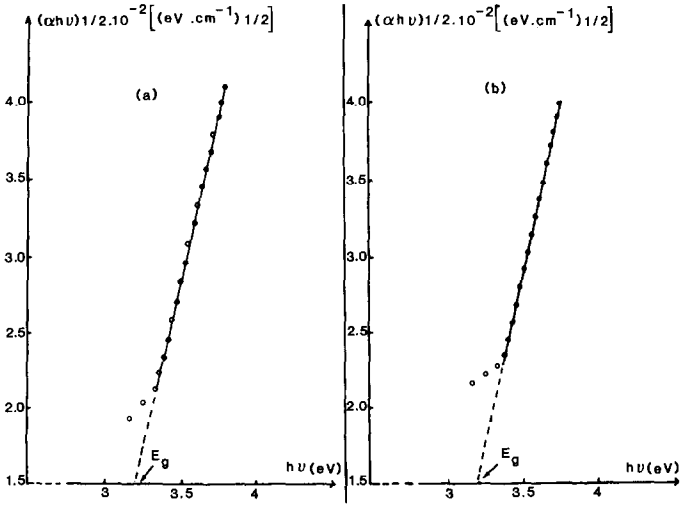


FIG. 5. Determination of the band-energy gap: (a) untreated films and (b) heat-treated films.

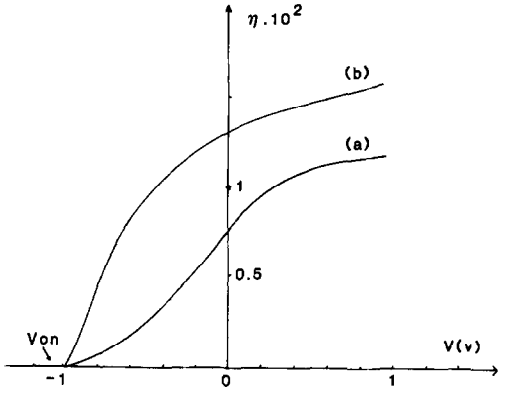


FIG. 6. Photocurrent efficiency vs potential curves for $SrTiO_3$ thin films: (a) untreated films and (b) heat-treated films.

$$|\ln(1-\eta)|^2 = \frac{2\alpha^2\varepsilon_r'\varepsilon_0}{qN_D}(V - V_{fb}), \quad (3)$$

where $V$ is the electrode potential and $N_D$ the ionized donor density; the other parameters are assigned their usual symbols.

Figures 6 and 7 show respectively the $\eta$ vs $V$ curves and the $|\ln(1-\eta)|^2$ vs $V$ curves deduced for $\lambda = 380$ nm, i.e., for $h\nu = 3{,}26$ eV, a value close to $E_g$.

As expected, the extrapolated $V_{fb}$ value (−1.0 V) is consistent with the photocurrent-onset potential $V_{on}$ (Table I). It is more positive than the values obtained for single crystal or for pelletized polycrystalline Sr $TiO_3$ (−1.30 V). This implies that some surface states are present at the film–electrolyte interface.

The ionized donor density calculated

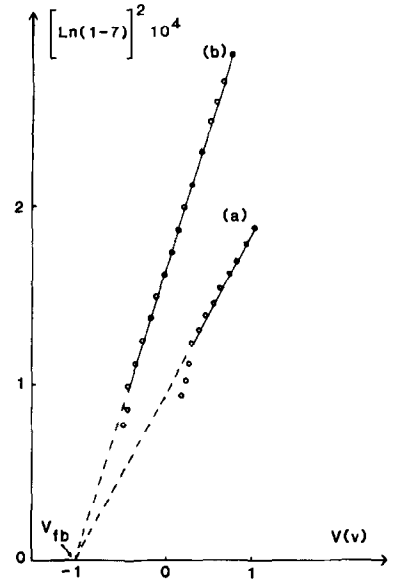


FIG. 7. $|\ln(1-\eta)|^2$ vs potential plots at $\lambda = 370$ nm: (a) untreated films and (b) heat-treated films.

from the slope of the straight lines is high ($N_D = 2.6 \times 10^{20}$ cm$^{-3}$), close to the electronic densities in the conduction band determined previously (*2*) (Table I). Such values characterize a degenerate semiconductor ($n^+$) and are responsible for a very narrow depletion layer, which is almost 100 times lower than the inverse of the absorption coefficient (Table I). That is consistent with Hodes's model, according to which the protective layer deposited on the Si-semiconductor behaves as a degenerate semiconductor (*1*).

TABLE I

EXPERIMENTAL PARAMETERS FOR UNTREATED AND HEAT-TREATED $SrTiO_3$ DEPOSITS

| | $\sigma$ (25°C)* ($10^{-3}$ $\Omega^{-1}$ cm$^{-1}$) | * $\varepsilon'$(25°C) | $\alpha$ (380 nm) $10^{+4}$ cm$^{-1}$ | $E_g$ (eV) | $\Delta E$* (±0.02 eV) | $n$* ($10^{20}$ e$^{\ell}$ cm$^{-3}$) | $V_{fb}$, $V_{on}$ (V) | $N_D$ ($-10^{20}$ cm$^{-3}$) | $\mu_e$ ($10^{-4}$ cm$^2$ V$^{-1}$ sec$^{-1}$) | $W$ at 0.5 V ($10^{-7}$ cm) |
|---|---|---|---|---|---|---|---|---|---|---|
| Untreated films | 5 | 100 | 1.45 | 3.2 | 0.13 | 1.2 (0.8) | −1 | 2.6 | 1.2 | 10 |
| Heat-treated films | 50 | 180 | 1.65 | 3.2 | 0.09 | 5 (4) | −1 | 2.6 | 12 | 8 |

* See ref. (*2*).

As observed for ITO films the conduction band electron density is high, but $V_{fb}$ (Sr $TiO_3$) is lower than that of ITO and should characterize a lower electron affinity (*1*). Consequently, the *n*-$SrTiO_3$ films should be used rather than ITO for protection against corrosion in aqueous solutions of efficient *p*-type semiconductors such as silicon. The adequate $V_{fb}$ value should indeed give rise to a high band bending at the semiconductor/film interface.

Such composite electrodes are presently under investigation in this laboratory.

## References


1. G. HODES, L. THOMPSON, J. DUBOW, AND K. RAJESHWAR, *J. Amer. Chem. Soc.* **105,** 324 (1983).
2. G. CAMPET, M. CARRERE, S. Z. WEN, C. PUPRICHITKUN, J. SALARDENNE, AND J. CLAVERIE, *Thin Solid Films,* submitted for publication.
3. O. S. HEAVENS, "Optical Properties of Thin Solid Films," Dover, New York (1965).
4. B. T. CHANG, G. CAMPET, J. CLAVERIE, P. HAGENMULLER, AND J. B. GOODENOUGH, *J. Solid State Chem.* **49,** 247 (1983).
5. E. A. DAVIS, AND N. F. MOTT, *Philos. Mag.* **24,** 1281 (1971).
6. E. J. JOHNSON, *in* "Semiconductors and Semimetals" (R. H. Williardson and A. C. Beer, Eds., Vol. 3, Chap. 6, Academic Press, New York (1967).
7. Y. MARFAING, "Photoconductivity, Photoelectric Effects: Handbook of Semiconductors," Vol. 2, North-Holland, Amsterdam (1980).
8. M. A. BUTLER, *J. Electrochem. Soc.* **128,** 200 (1981).
9. W. W. GÄRTNER, *Phys. Rev.* **116,** 84 (1959).
10. The investigations have been supported by GRECO 130061 of CNRS.